

The Buried Oxide Properties in Oxygen Plasma-Enhanced Low-Temperature Wafer Bonding

Y. H. Wu,^a C. H. Huang,^a W. J. Chen,^b C. N. Lin,^{a,c} and Albert Chin^a

^aDepartment of Electronics Engineering, National Chiao Tung University, Hsinchu, Taiwan

^bDepartment of Mechanical Materials Engineering, National Huwei Institute, Huwei, Taiwan

^cUnited Microelectronics Corporation, Hsinchu, Taiwan

We have studied the buried oxide integrity in oxygen plasma-enhanced low-temperature wafer bonding. As observed by cross-sectional scanning electron microscopy, the bonding strength of the oxygen plasma-treated sample is so large that forced separation for a 600°C bonded wafer takes place at the heterointerface of the thermal oxide and the Si substrate rather than at the oxide-oxide bonding interface. The plasma-enhanced bonding shows good structure property with negligible defects as observed by cross-sectional transmission electron microscopy. From capacitance-voltage measurement, good electrical property is evidenced by the low oxide-charge and interface-trap densities of $-2.0 \times 10^{10} \text{ cm}^{-2}$ and $3 \times 10^{10} \text{ eV}^{-1} \text{ cm}^{-2}$, respectively, from capacitance-voltage measurements.

© 2000 The Electrochemical Society. S0013-4651(99)11-083-8. All rights reserved.

Manuscript submitted November 22, 1999; revised manuscript received April 11, 2000.

Wafer bonding has attracted much attention recently because of the important application in micro-electrical-mechanical systems (MEMS)¹⁻³ and silicon-on-insulator (SOI) technology.⁴⁻¹¹ In comparison to separation by implanted oxygen (SIMOX), the bond and etchback SOI (BESOI) generally has few buried oxide defects,⁶ which is important for device and circuit applications. Furthermore, thick buried oxide can be easily formed by BESOI, which is useful for radio frequency (rf) or power devices because of the lower substrate loss and better isolation.¹² However, one minor drawback for wafer bonding is the required high temperature and long annealing time necessary to increase the bonding strength for subsequent fabrication. Recently, a low thermal budget bonding process has been proposed that may overcome this problem using oxygen plasma pretreatment.¹³⁻¹⁵ The plasma treatment can enhance the number of OH groups at the surface by an order of magnitude and greatly improve bonding strength.¹⁴ Plasma-induced surface charges may also enhance the oxide growth rate at the bonding interface, increase atom mobility in the surface region, and reduce free energy of oxide formation by radical reactant ions.¹⁵ However, plasma-induced defects may influence oxide integrity¹⁶⁻¹⁹ which is important for further device process. In this paper, we have studied buried oxide integrity using oxygen plasma-enhanced wafer bonding, followed by a 600°C annealing with negligible impurity out-diffusion at this low temperature.³ The bonding interface shows good structural properties as observed by cross-sectional scanning electron microscopy (SEM) and transmission electron microscopy (TEM). Good electrical properties are also observed by the low oxide-charge density of $-2.0 \times 10^{10} \text{ cm}^{-2}$ from capacitance-voltage (C-V) measurement. These results suggest that plasma pretreatment is suitable for low-temperature oxide bonding applications.

Experimental

Standard 4 in. Si(100) wafers were used in this experiment. Wet oxides of 1060 Å were grown on each wafer at 850°C. The standard RCA cleaning process was used to achieve a hydrophilic condition. One wafer set was exposed to oxygen plasma in a reactive ion etcher (RIE) for 4 min before initial contact and the other wafer set without plasma treatment was also studied as a reference. The oxygen plasma conditions were 50 W power and 20 sccm oxygen flow with a pressure of 20 mTorr. Initial bonding was performed in atmosphere at room temperature. Thermal bonding was performed at 600°C in nitrogen ambient for 15 h. Cross-sectional SEM and TEM were used to examine the material properties of bonding. To further investigate the effect of oxygen plasma treatment, we forced the bonded wafers to separate at the edge of the wafer using a sharp knife. Metal-oxide semiconductor (MOS) capacitors were fabricated by Al deposition

and patterning on bonded oxide after forced separation. C-V measurements were used to characterize the electrical properties of the plasma effect on the bonded oxide.

Results and Discussion

Figure 1a and b shows the cross-sectional SEM of the separated wafer without and with the oxygen plasma treatment, respectively. As shown in Fig. 1a, the separated wafer has a measured oxide thickness of 1100 Å that is almost identical to the original oxide thickness before bonding, within experimental error. Therefore, there is no bonding or chemical reaction after the 600°C thermal treatment. This is also consistent with the reported results in literature that a high temperature of $\sim 1100^\circ\text{C}$ is required to form strong chemical bonding.¹¹ In sharp contrast to the one without oxygen plasma treatment, the separated wafers shown in Fig. 1b have a thicker oxide on one of the wafers and no measurable oxide on other part of the bonded wafer. The measured oxide thickness on the one with thick oxide is 2130 Å, twice the thickness of the initial oxide. The observed thin white line in the middle of the thick oxide may be due to oxygen plasma treatment. We also examined the bonding by cross-sectional SEM in an air-bubbled region. As shown in Fig. 1c, the oxide thickness gradually decreased from the bonded region to the air-bubbled region with twice the thickness of the original oxide in the bonded region. Therefore, successful bonding can be formed by oxygen plasma treatment even at 600°C annealing. As observed by microscope, the thermal oxide of one wafer is stripped off and attached to the other wafer after forced separation. Thus, the bonding strength is so large that forced separation did not happen at the oxide-oxide bonding interface. Instead, the separation occurred at the thermal oxide-Si substrate heterointerface. The surface roughness after separation is measured from cross-sectional TEM and the root mean square (rms) roughness is 2 Å. Such strong bonding can only be obtained by conventional methods after a high-temperature annealing at $\sim 1100^\circ\text{C}$ where a viscous flow of oxide occurs at this temperature.¹¹

We have used cross-sectional TEM to further study the oxygen plasma-treated wafer bonding. As shown in Fig. 2, there is no defect in bonded oxide that can be observed. A tiny region at the middle of the bonded wafer is also found that is consistent with the observed thin white line by SEM. Because the tiny region has a different contrast as compared with nearby oxide, this is an indication of a slightly different material property from conventional thermal oxide. Although a detailed mechanism of oxygen plasma treatment is still not well known, the high-energy plasma may damage the oxide to break the Si-oxide bonds and create traps. It may also form oxygen-rich oxide after oxygen plasma treatment. In either case, the oxygen plasma-treated oxide can enhance the bonding strength, but the oxide

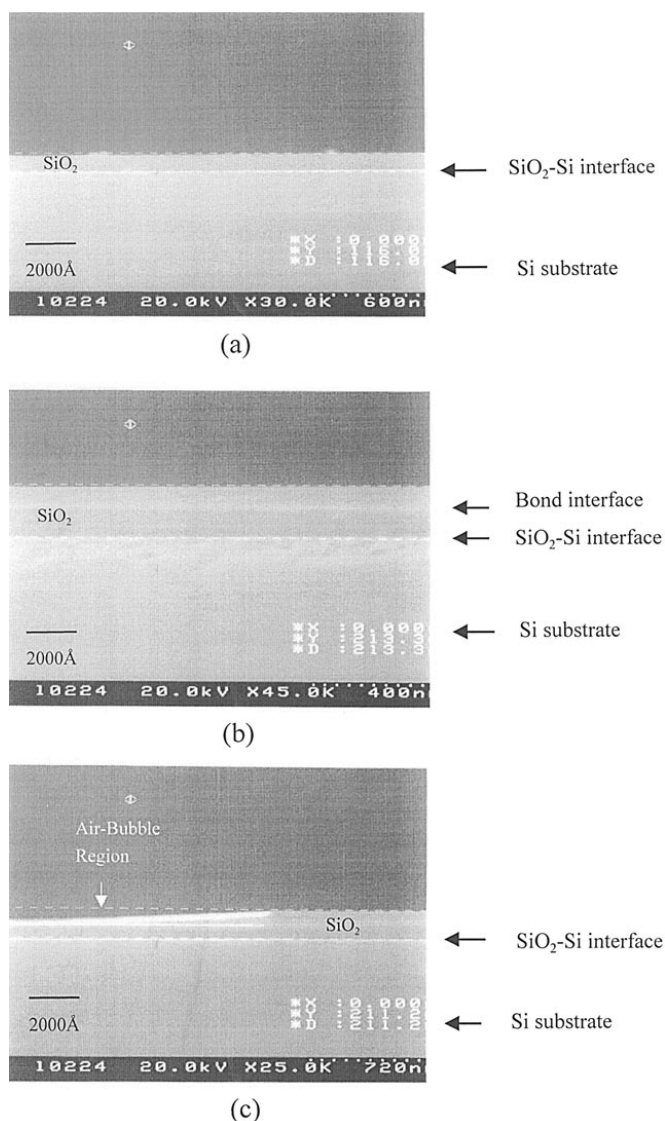


Figure 1. Cross-sectional SEM of bonded wafer with forced break in (a) bonded region without oxygen plasma treatment, (b) bonded region with oxygen plasma treatment, and (c) air-bubble region with oxygen plasma treatment. Oxygen plasma treatment is used before thermal annealing. The bonding conditions are 600°C thermal annealing for 15 h.

property may also be slightly changed from original thermal oxide and show a different contrast in TEM.

To further characterize the electrical properties of bonded oxide using oxygen plasma pretreatment, we fabricated MOS capacitors directly on these oxides in Fig. 1b after forced separation. Figure 3 shows the measured high- and low-frequency C-V curves. Oxide charge and interface trap densities can be directly derived from this data. Very low oxide charge and interface trap densities of $-2.0 \times 10^{10} \text{ cm}^{-2}$ and $3 \times 10^{10} \text{ eV}^{-1} \text{ cm}^{-2}$, respectively, are obtained, which indicates good oxide properties are still maintained even after oxygen plasma treatment. The interface trap density (D_{it}) is derived from the formula

$$D_{it} = C_{it}/qA = \frac{\left(\frac{1}{C_q} - \frac{1}{C_{ox}}\right)^{-1} - \left(\frac{1}{C_h} - \frac{1}{C_{ox}}\right)^{-1}}{qA} \quad [1]$$

where C_q is quasi-static capacitance and C_h is high-frequency capacitance. The oxide charge is obtained from the flatband

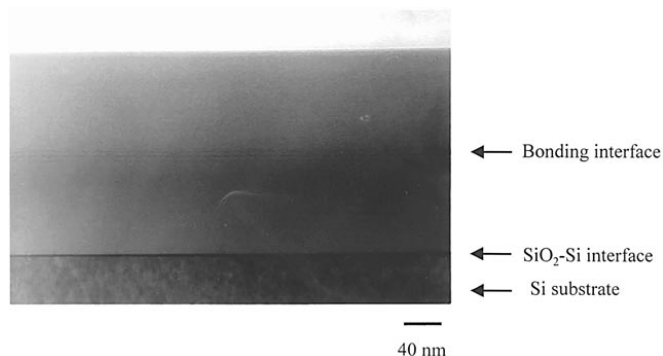


Figure 2. Cross-sectional TEM of the bonded region with oxygen plasma treatment after forced break.

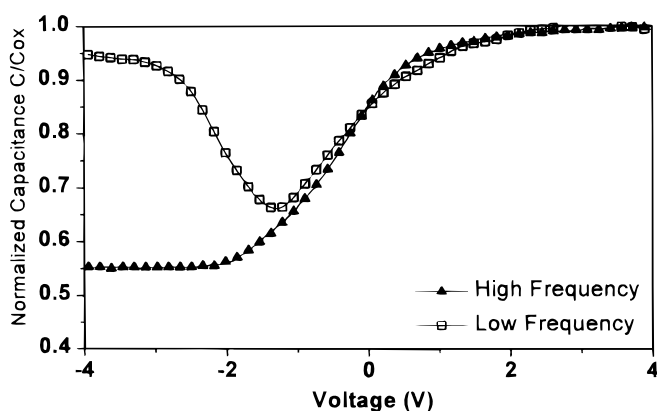


Figure 3. Low- and high-frequency C-V curves of the initial bonded oxide.

$$V_{FB} = \Phi_{MS} - \frac{Q_0}{C_{ox}} \quad [2]$$

Where Q_0 is fixed oxide charge and Φ_s is the workfunction difference between n^+ -poly and Si substrate.

The measured negative charge density, in contrast to normally observed positive value, may be due to trapped electrons by oxygen plasma. Other possibilities may be due to oversaturated hydrogen in oxide by hydrophilic bonding surface proposed by Afanas'ev *et al.*²⁰

To further investigate the origin of negatively charged oxide, we grew an additional 40 Å oxide on top of bonded oxide followed by the same capacitor fabrication process. This additional 40 Å oxide was thermally grown by dry O_2 at 900°C for 5.5 min. Figure 4 shows the measured C-V curves, and the important oxide properties are summarized in Table I. The additional oxidation shows little effect on

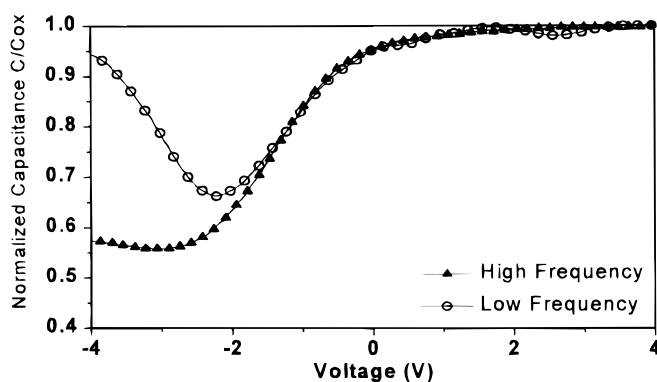


Figure 4. Low- and high-frequency C-V curves of the bonded oxide after growth of a 40 Å thermal oxide.

Table I. Oxide properties comparison between initial bonded and additional 40 Å oxides.

Oxide property	Oxide charge density (cm ⁻²)	Interface trap density (eV ⁻¹ cm ⁻²)
Initial bonded oxide	-2×10^{10}	3×10^{10}
Additional 40 Å oxidation	6×10^{10}	4×10^{10}

interface property, and the good interface property is evidenced by the close values of high- and low-frequency C-V curves around accumulation. This good interface property is due to the large distance from the oxygen plasma to the interface. The low interface charge density is important for achieving a low noise for devices fabricated on SOI. On the contrary, a clear shift of flatband voltage is observed after additional oxidation. Because of the very thin extra thickness of additional oxide, the large flatband shift is due to different oxide charges. The additional oxidation also changes the oxide charge density from negative to conventionally measured positive values. Therefore, this result suggests that the negatively charged oxide originated from the oxygen plasma treatment. However, in spite of the negative value, the density of oxide charge is very low, which shows good electrical quality of buried oxide with plasma-enhanced bonding.

Conclusion

In conclusion, we studied the buried oxide integrity using oxygen plasma-enhanced low-temperature wafer bonding. The bonding strength of the oxygen plasma-treated sample was so large that forced separation took place at the thermal oxide-Si substrate heterointerface instead at the oxide-oxide bonding interface. Very low oxide charge and interface trap densities of -2.0×10^{10} cm⁻² and 3×10^{10} eV⁻¹ cm⁻², respectively, are obtained, which indicates that the good oxide properties were still maintained even after oxygen plasma treatment.

Acknowledgment

We are thankful for helpful discussions with Professor K. C. Hsieh at the Department of Electrical Engineering, University of Illinois, and for continuous support from Dr. C. Tsai and Professor T. F. Lei at our Department. This work has been supported in part by NSC (88-2215-E-009-032) of Taiwan.

The National Chiao Tung University assisted in meeting the publication costs of this article.

References

1. D. Xiaoyi, W. H. Ko, in *Int. Solid-State Sen. Actuators, Tech. Dig.*, 201 (1991).
2. D. Xiaoyi, W. H. Ko, and J. M. Mansour, *Sens. Actuators A*, **A23**, 866 (1990).
3. A. Chin, K. Lee, Y.-C. Huang, Y.-S. Lin, and W. Hsu, in *Micro System Technologies, Tech. Dig.*, 233 (1996).
4. P. C. Yang and S. S. Li, *Appl. Phys. Lett.*, **61**, 1408 (1992).
5. H. S. Chen and S. S. Li, *IEEE Trans. Electron Devices*, **ED-39**, 1740 (1992).
6. W. P. Maszara, Extended Abstract in *Int. Solid State Mater.*, 294 (1998).
7. J. B. Lasky, *Appl. Phys. Lett.*, **48**, 78 (1986).
8. M. Shimbo, K. Furukawa, K. Fukuda, and K. Tanzawa, *J. Appl. Phys.*, **60**, 2987 (1986).
9. N. Sato and T. Yonehara, *Appl. Phys. Lett.*, **65**, 1924 (1994).
10. K. Sakaguchi, N. Sato, K. Yamagata, and Y. Fujiyama, *Jpn. J. Appl. Phys.*, **2B**, 842 (1995).
11. W. P. Maszara, G. Goetz, A. Caviglia, and J. B. McKitterick, *J. Appl. Phys.*, **64**, 4943 (1988).
12. A. Chin, D. Prinslow, V. Tsai, G. Nasserbakht, and B. Eklund, in *Int. Symp. VLSI-TSA, Tech. Dig.*, 148 (1997).
13. G. L. Sun, J. Zhan, Q. Y. Tong, S. J. Xie, Y. M. Cai, and S. J. Lu, *J. Phys. C.*, **49**, 79 (1988).
14. G. Kissinger and W. Kissinger, *Sens. Actuators A*, **A36**, 149 (1993).
15. S. N. Farrens, J. R. Dekker, J. K. Smith, and B. E. Roberds, *J. Electrochem. Soc.*, **142**, 3949 (1995).
16. A. Chin, B. C. Lin, W. J. Chen, Y. B. Lin, and C. Tsai, *IEEE Electron Device Lett.*, **EDL-19**, 426 (1998).
17. A. Chin, C. C. Liao, C. H. Lu, W. J. Chen, and C. Tsai, in *Symp. VLSI Tech.*, 135 (1999).
18. B. C. Lin, Y. C. Cheng, A. Chin, T. Wang, and C. Tsai, Extended Abstract in *Int. Solid State Mater.*, 110 (1998).
19. J. M. Lai, W. H. Chieng, B. C. Lin, A. Chin, and C. Tsai, *J. Electrochem. Soc.*, **146**, 2216 (1999).
20. V. Afanas'ev, P. Ericsson, S. Bengtsson, and M. O. Andersson, *Appl. Phys. Lett.*, **66**, 1653 (1995).